

## Highly monodisperse vinyl functionalized silica spheres and their self-assembled three-dimensional colloidal photonic crystals

Tian-Song Deng, Jun-Yan Zhang, Kong-Tao Zhu, Qi-Feng Zhang, Jin-Lei Wu\*

Key Laboratory for the Physics and Chemistry of Nanodevices, Department of Electronics, Peking University, Beijing 100871, People's Republic of China

### ARTICLE INFO

#### Article history:

Received 13 August 2009

Received in revised form 7 December 2009

Accepted 22 December 2009

Available online 6 January 2010

#### Keywords:

Monodisperse

Vinyl functionalized silica spheres

Self-assembled

Colloidal photonic crystals

### ABSTRACT

A one-step method was presented for the controlled synthesis of highly monodisperse vinyl functionalized silica spheres (VFSSs), which could be self-assembled into three-dimensional (3D) *fcc* colloidal photonic crystals on a horizontal glass slide by a gravity sedimentation process. One precursor (vinyltriethoxysilane) and one solvent (water) were used in the experiment. The size of VFSSs could be adjusted from 420 to 650 nm with relative standard deviation below 2% by controlling the dripping speed of diluted ammonia catalyst, without changing the concentration of precursor/catalyst. SEM and TEM images illustrate the copiousness in quantity and the uniformity in size/shape of the VFSSs.  $^{29}\text{Si}$  nuclear magnetic resonance (NMR) spectrum confirms the surfaces of VFSSs have abundant vinyl groups ( $-\text{CH}=\text{CH}_2$ ) which connect to the silicon atoms. Optical characterizations of the transmission spectra reveal that the periodic arrays exhibit a photonic band gap in the (1 1 1) direction of the *fcc* lattice in consistent with the Bragg diffraction theory. This work has also been extended to prepare other monodisperse surface-modified silica spheres and fabricate organic functionalized colloidal templates.

© 2010 Elsevier B.V. All rights reserved.

### 1. Introduction

Since Yablonovich and John firstly proposed the concept of photonic crystal independently in 1987 [1,2], design and fabrication of colloidal photonic crystals with 3D regular periodicity of dielectric structures have attracted considerable attention [3–5]. Colloidal photonic crystals, which diffract light in UV, visible, and near-infrared regions, can control the propagation of light [6–9]. Usually, colloidal photonic crystals are fabricated by using monodisperse silica or polystyrene spheres [10]. They are widely used as templates to fabricate inverse opal periodic arrays which have more promising optical properties [11–14]. Preparation of highly monodisperse colloidal spheres and controlling the size dimension of colloidal spheres are critical for a good assembly in the preparation of colloidal photonic crystals [15,16]. Stöber et al. [17] first successfully synthesized the monodisperse pure silica spheres by controlled hydrolysis of the tetraethyl orthosilicate (TEOS) in ethanol solution using ammonia as a catalyst (Stöber method). This technique is extensively used but the resulted particle size dimensions are limited and the surface properties are inanimate. To increase the particle size and modify the surface properties of the colloidal photonic crystals, most studies have focused on the surface functionalization on the pure silica spheres [18–25].

During the synthesis, the starting mixtures often include different triethoxysilanes (RTES) or trimethoxysilanes (RTMS), where the organic substitute R was varied from methyl, phenyl, octyl to vinyl [22–24]. However, the reaction systems are too complex while using ethanol/methanol-water based systems or adding some surfactants, and the precursors commonly contain two materials (silane and TEOS) [22,25]. The procedures need two or even more inconvenient processes [18–24]. For example, Wang et al. [18–20] prepared monodisperse sub-micrometer silica spheres to fabricate near-infrared photonic crystals by modifying the surface of silica with organic groups. Recently, Hah et al. [26] have synthesized hollow hybrid silica particles using a sol-gel reaction without adding ethanol, and the precursor was only one material. Then some researchers extended this method [27,28]. But the resulted particles often have a large number of small spheres and the monodispersity of hybrid silica spheres were hard to control [28]. Furthermore, in most kind of the silanes, surfactant must be added [26–28].

We recently reported a method about one-step synthesis of monodisperse silica spheres functionalized by organic groups using a sol-gel process in aqueous solution. By controlling the concentration of the precursor and the catalyst, the particle size can be adjusted [29]. Compared to the traditional method, we used an organosilane as precursor and water as solvent, and no surface modification or addition of surfactant was necessary. Here, we report the extensive method for preparing highly monodisperse VFSSs which could be self-assembled into 3D *fcc* colloidal photonic crystals. The method has several main progresses. First, it

\* Corresponding author. Tel.: +86 10 62761333; fax: +86 10 62761333.  
E-mail addresses: [jacintazjy@pku.edu.cn](mailto:jacintazjy@pku.edu.cn) (J.-Y. Zhang), [ktzhu@pku.edu.cn](mailto:ktzhu@pku.edu.cn) (K.-T. Zhu), [qfzhang@pku.edu.cn](mailto:qfzhang@pku.edu.cn) (Q.-F. Zhang), [jlwu@pku.edu.cn](mailto:jlwu@pku.edu.cn) (J.-L. Wu).

well controls the size, uniformity and stability of VFSSs. The size of VFSSs ranging from 420 to 650 nm with relative standard deviation ( $\sigma_r$ ) below 2% were obtained only by adjusting the dripping speed of diluted ammonia catalyst, without changing the concentration of precursor/catalyst. Furthermore, the resulted VFSSs are highly monodisperse and easy to be self-assembled into 3D *fcc* colloidal photonic crystals on a horizontal glass slide by a gravity sedimentation process. The fabrication process is relatively simple and the obtained colloidal photonic crystals have a good optical property in consistent with Bragg diffraction theory.

## 2. Materials and methods

### 2.1. Materials and substrates

Vinyltriethoxysilane (VTES, 95%), ammonia solution ( $\text{NH}_3 \cdot \text{H}_2\text{O}$ , 25%), sulfuric acid (95%), hydrogen peroxide (30%) and ethanol were all purchased from Sinopharm Chemical Reagent Beijing Co., Ltd. All chemicals were used as received without further purification. Ultrapure water (18.2 M $\Omega$  cm) is used directly from a Milli-Q water system. Microscope slides (75 mm  $\times$  25 mm  $\times$  1 mm, Sail Brand, China) were cut into square pieces (12.5 mm  $\times$  12.5 mm  $\times$  1 mm).

### 2.2. Synthesis of highly monodisperse VFSSs

Highly monodisperse VFSSs were synthesized using a sol–gel reaction in aqueous solution according to a recent literature of us [29]. In a typical procedure for the preparation of VFSSs, 3 mL VTES was added in 50 mL  $\text{H}_2\text{O}$  under vigorous magnetic stirring (300 rpm) for  $\sim$ 2 h. Then the organic droplets were completely dissolved and a transparent solution was obtained. Ammonia was diluted with water (a volume ratio of ammonia:water = 1:4). Under the constant magnetic stirring rate, 1 mL diluted ammonia solution was consecutively added to the reaction mixture via a burette syringe and the reaction was allowed to proceed at room temperature for 1 h. The mixture contained 0.27 mol/L VTES and 0.20 mol/L  $\text{NH}_3$ . After the completion of the reaction, in order to remove impurities, such as ammonia, water, and unreacted VTES, the resulting particles were separated from the reaction medium by repeated centrifugation (3000 rpm) and ultrasonic dispersion (using ethanol) cycles, and then redispersed in ethanol for further usage.

Furthermore, in order to obtain different sizes of VFSSs, the dripping speed of diluted ammonia catalyst was changed in our studies. A burette syringe with a microsyringe needle was used to control the dripping speed of the diluted ammonia solution, which can precisely control the dripping speed ranging from a few drops per minute to hundreds of drops per minute. The standard of microsyringe needle was 0.5 mm  $\times$  20 mm (160 drops  $\approx$  1 mL, means 1 drop  $\approx$  0.00625 mL). The experimental details are listed in Table 1.

**Table 1**

Mean diameters ( $\bar{x}$ ) and relative standard deviation ( $\sigma_r$ )<sup>a</sup> of VFSSs obtained under different dripping speed of diluted ammonia solution.

Sample	VTES (mL)	Diluted $\text{NH}_3^b$ (mL)	Dripping speed (drops/min)	Dripping time (s)	$\bar{x}$ (nm)	$\sigma_r$ (%)
1	3	1	30	320	649	1.13
2	3	1	40	240	553	1.56
3	3	1	60	160	495	1.08
4	3	1	90	107	455	1.62
5	3	1	160	60	423	1.45

<sup>a</sup> The mean diameters ( $\bar{x}$ ) and relative standard deviation ( $\sigma_r$ ) of silica spheres are defined by statistics.  $\bar{x} = \sum_{i=1}^n x_i/n$ ,  $\sigma = \sqrt{\sum_{i=1}^n (x_i - \bar{x})^2 / (n - 1)}$  ( $n > 5$ ),  $\sigma_r = (\sigma/\bar{x}) \times 100\%$ , where  $x_i$  is the diameter gained by measuring  $n$  spheres (about two hundred) for each sample using SEM,  $\bar{x}$  is the mean diameter,  $\sigma$  is the standard deviation and  $\sigma_r$  is the relative standard deviation.

<sup>b</sup> Ammonia, a high volatile material, was diluted with water (a volume ratio of ammonia:water = 1:4).

### 2.3. Fabrication of colloidal photonic crystals

Glass slides were rinsed with running water, ultrasonicated for 30 min in acetone. Then, they were washed with distilled water, and then ultrasonicated for 1 h in piranha solution (a mixture of 70% sulfuric acid and 30% hydrogen peroxide. WARNING: The above solution reacts violently with organic materials. Handle with caution). The substrates were finally rinsed with deionized water and dried with a stream of nitrogen. Colloidal photonic crystals were prepared from the VFSSs using a sedimentation self-assembled process. Several as-prepared glass slides were set on the bottom of a beaker. The beaker was placed in an oil bath at 60 °C. A certain amount of the VFSSs dispersions (volume fraction 1%) was dropped onto the glass slide, and spread uniformly on the whole region of the substrate spontaneously. As the solvent (ethanol) evaporated, the uniform film was obtained with domain size typically in the range of several hundred microns. To evaluate the effect of the evaporation temperature on the crystalline quality of colloidal photonic crystals, samples were fabricated at different temperatures (40 °C, 60 °C, and 80 °C, the fabricating times were 200 s, 60 s, and 20 s, respectively).

### 2.4. Characterization of VFSSs and their colloidal photonic crystals

The morphology was observed using an environmental scanning electron microscope (ESEM) (FEI Quanta200FEG) and transmission electron microscope (TEM) (HITACHI H-9000NAR). For ESEM, the accelerating voltage was 15 kV, and the pressure of the chamber was 0.90 Torr. For TEM, the accelerating voltage was 300 kV. The sizes of the VFSSs were measured using ESEM (about two hundred spheres for each sample).

The solid-state  $^{29}\text{Si}$  CP-MAS (CP: cross polarization, MAS: magic angle spinning) NMR spectra of VFSSs were carried out on a Bruker AV 300 spectrometer. The optical transmission spectra were obtained on a UV–VIS–NIR Recording Spectrophotometer (SHIMADZU UV-3100). A home-made mask was used to constrain the incident light into a 1 mm diameter circle.

## 3. Results and discussion

### 3.1. Morphology and structural characterization of VFSSs

Fig. 1 shows the SEM and TEM images of a typical sample prepared using sol–gel process. The sample was synthesized with dripping speed of 60 drops/min. The SEM image in Fig. 1a clearly illustrates the abundance in quantity and the uniformity in size/shape that could be routinely accomplished in this synthesis. The TEM image in Fig. 1b reveals that the surfaces of these colloids were spherical and smooth. It must be noted that the as-prepared spheres are solid (not-hollow). We can see the color of each single sphere is uniform, and the overlaps are darker than the color of a single sphere. It confirms that the spheres are solid spheres.

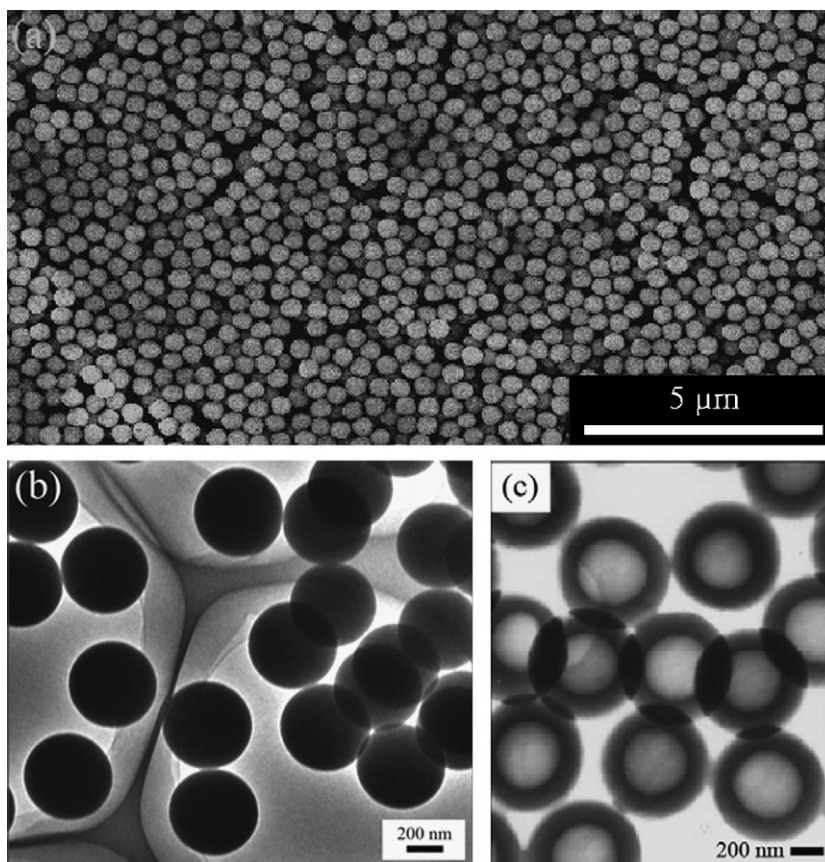


**Fig. 1.** (a) SEM and (b) TEM images of VFSSs (495 nm in mean diameter) fabricated by 3 mL VTES and 50 mL H<sub>2</sub>O by adding 1 mL diluted ammonia solution with a dripping speed of 60 drops/min. The reaction was carried out under constant stirring rate at room temperature (22 ± 1 °C). (c) TEM image of monodisperse hollow silica particles functionalized with phenyl groups [26]. Copyright 2003 Royal Society of Chemistry.

This is as different as Hah's result (Fig. 1c) [26]. In Fig. 1c for each single sphere, the external part was dark and the internal part was white. We can observe a noticeable contrast between the core and the shell of the particles in Fig. 1c. Hah et al. [26] obtained phenyl functionalized hollow silica particles using a two-step method: the hydrolysis of phenyltrimethoxysilane (PTMS) was performed under acidic conditions; the condensation of the silane progressed under alkaline conditions. We do not need acidic conditions in the whole processes. It is clear that our synthetic hybrid silica spheres are more spherical and uniform compared with their results.

The solid-state <sup>29</sup>Si CP-MAS NMR spectrum of VFSSs is shown in Fig. 2. According to the literatures [30–32], the T species originate from the monomer, where the silicon atom is coordinated by three

oxygen atoms (T<sup>x</sup>: RSiO<sub>x</sub>(OH)<sub>3-x</sub>, R: organic group). The Q species originate from TEOS, in which the silicon atom is coordinated by four oxygen atoms (Q<sup>x</sup>: SiO<sub>x</sub>(OH)<sub>4-x</sub>). In our experiment, the T species originate from the VTES, having four classes of T species: T<sup>0</sup> (CH<sub>2</sub>=CHSi(OH)<sub>3</sub>), T<sup>1</sup> (CH<sub>2</sub>=CHSi(OH)<sub>2</sub>), T<sup>2</sup> (CH<sub>2</sub>=CHSi(OH)(OH)), and T<sup>3</sup> (CH<sub>2</sub>=CHSiO<sub>3</sub>).

The <sup>29</sup>Si NMR spectrum shows two peaks of T species, due to T<sup>2</sup> (-70.5 ppm) and T<sup>3</sup> (-79.6 ppm). Fig. 3 indicates the Jain's work [33]. They used two steps to modify the surface of silica with vinyl groups. Only Q species' peaks appeared in pure silica, and VTES-grafted PP/silica had both the Q and T species (see Fig. 3). But the intensity of Q species was stronger than the T species, indicating that the quantity of vinyl groups was limited. In our one-step direct synthesis of VFSSs, only T<sup>2</sup> and T<sup>3</sup> peaks appeared in the <sup>29</sup>Si NMR spectrum, indicating that the surface had abundant vinyl groups. Moreover, the area of T<sup>3</sup> unit was about 3.5 times of T<sup>2</sup> unit's. It provided another important proof that a majority of OH groups were replaced by CH=CH<sub>2</sub> groups in the hybrid silica spheres. The results are consistent with FT-IR analysis. The FT-IR spectrum confirms that the vinyl group (-CH=CH<sub>2</sub>) exists and connects to the silicon atom in the hybrid silica [29].

### 3.2. Control over the size of VFSSs

Generally, the size of hybrid silica spheres depends on a number of parameters that include, for example, the concentration of VTES precursor/ammonia catalyst, the ratios of water and VTES, the stirring rate, the temperature, and the reaction time. We discussed the reaction time and the concentration of VTES precursor/ammonia catalyst in the previous researches. The increasing of the precursor

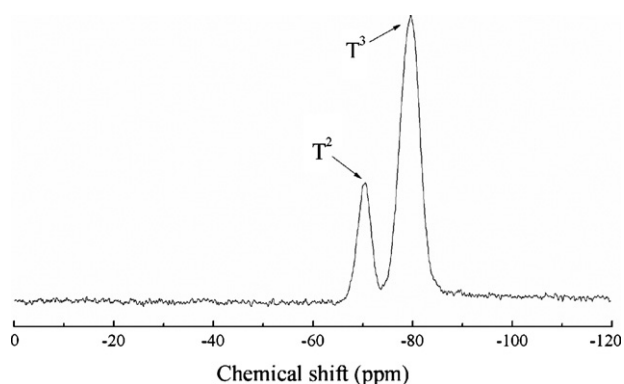


**Fig. 2.** Solid-state <sup>29</sup>Si CP-MAS NMR spectrum of VFSSs.



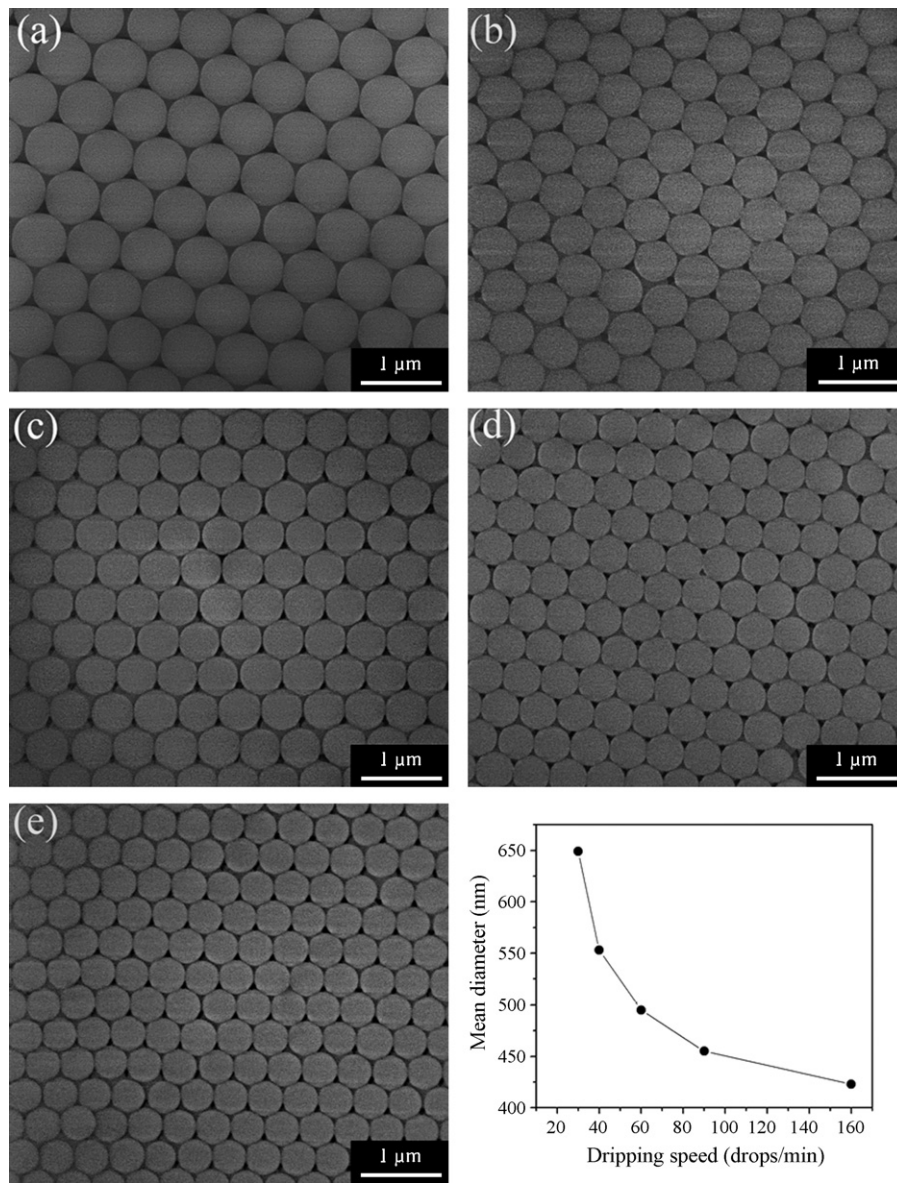


**Fig. 4.** SEM images of monodisperse VFSSs prepared using 3 mL VTES and 1 mL diluted ammonia solution (a volume ratio of ammonia:water = 1:4) in 50 mL H<sub>2</sub>O by various dripping speed of diluted ammonia catalyst: (a) 30 drops/min, (b) 40 drops/min, (c) 60 drops/min, (d) 90 drops/min, and (e) 160 drops/min, respectively. The resultant particle sizes are (a) 649 nm, (b) 553 nm, (c) 495 nm, (d) 455 nm, and (e) 423 nm. The reaction was carried out under constant stirring rate at room temperature ( $22 \pm 1^\circ\text{C}$ ). Samples of the colloidal photonic crystals were fabricated on a horizontal glass slide at  $60^\circ\text{C}$  evaporation temperature. The plot shows that the particle size decreases with the increase of the dripping speed of diluted ammonia catalyst.

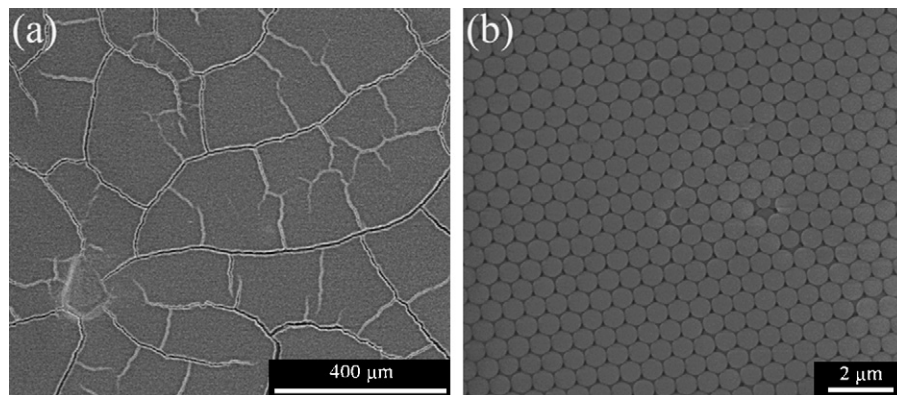


**Fig. 5.** SEM images of (a) low magnification and (b) higher magnification self-assembled colloidal photonic crystals on a horizontal glass slide. The mean diameter of VFSSs is 649 nm. Samples were fabricated at  $60^\circ\text{C}$  evaporation temperature.

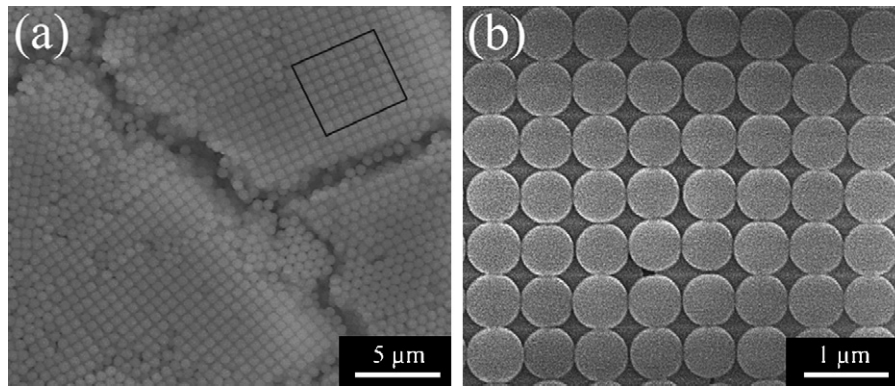


**Fig. 6.** SEM images of self-assembled colloidal photonic crystals, square arrangement can be observed: (a) low magnification, the schematic rectangular region shows the {100} type plane; (b) higher magnification. The mean diameter of VFSSs is 649 nm. Samples were fabricated on a horizontal glass slide at 60 °C evaporation temperature.

### 3.4. Optical properties of colloidal photonic crystals

As is widely described elsewhere, UV–VIS–NIR spectroscopy is an interesting technique for characterizing the optical properties of such colloidal photonic crystals [39,40]. We have examined optical properties of the 3D colloidal photonic crystals by measuring their transmission spectra with a UV–VIS–NIR recording spectrophotometer (UV-3100, Shimadzu).

Fig. 8 shows transmission spectra of the as-prepared 3D colloidal photonic crystals with different particle sizes. When the particle size is 423 nm, the absorption peak (photonic stop band) at 934 nm can be observed. With a further increase in particle size to 455 nm, 495 nm, 553 nm, and 649 nm, the absorption peak shifts to 980 nm, 1083 nm, 1224 nm, and 1416 nm, respectively. An approximate expression for the absorption maxima position is given by the modified form of Bragg's law (Eq. (1)), which takes into account the reduced angle with respect to the normal that light experiences on entering a medium with average refractive index  $n_{\text{eff}}$ , i.e., taking into account Snell's law of refraction [39,40]

$$m\lambda = 2d_{hkl}(n_{\text{eff}}^2 - \sin^2\theta)^{1/2} \quad (1)$$

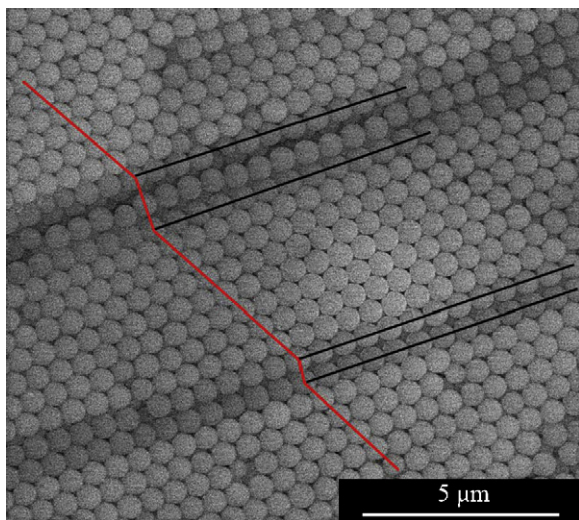


**Fig. 7.** SEM image of colloidal photonic crystals composed of VFSSs with a diameter of 649 nm. Samples were fabricated on a horizontal glass slide at 60 °C evaporation temperature. The red marked lines indicated different arrayed directions. And the black marked lines (terraces) are either {111} type or {100} type plane. (For interpretation of the references to color in this figure legend, the reader is referred to the web version of the article.)

where  $m$  is an integer (corresponding to the diffraction order).  $\lambda$  is the Bragg diffracted wavelength,  $d_{hkl}$  is the distance between two consecutive lattice planes with Miller indices  $(h, k, l)$ ,  $n_{\text{eff}}$  is the effective refractive index of the crystal, and  $\theta$  is the incidence angle.

In our experimental conditions, the incidence light was perpendicular to the surface of the films ((111) facet) in all of the measurement. Thus, the incidence angle  $\theta = 0^\circ$ , and the Miller indices  $(h, k, l) = (1, 1, 1)$ . Eq. (1) can be modified as

$$\lambda_{\text{max}} = 2d_{111}n_{\text{eff}} \quad (2)$$

where  $\lambda_{\text{max}}$  means the maxima absorption peak, set  $m = 1$ . For an fcc lattice with unit cell parameter  $a$ , the interplanar spacing  $d_{111}$  is given by:

$$d_{hkl} = \frac{a}{(h^2 + k^2 + l^2)^{1/2}}$$

The relationship between the unit cell parameter  $a$  and the particle size  $D$  is given by  $a = \sqrt{2}D$ , thus we can get

$$d_{111} = \sqrt{\frac{2}{3}}D \quad (3)$$

And the effective refractive index  $n_{\text{eff}}$  is calculated using indices of silica ( $n_s = 1.445$ ) and air ( $n_a = 1$ ), and the volume fraction  $f$  (74% for ideal close-packed spheres) occupied by the silica spheres accord-

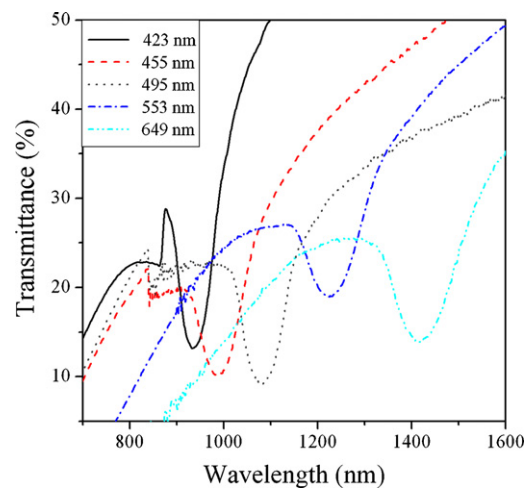


**Fig. 8.** Transmission spectra at normal incidence for colloidal photonic crystals prepared with different sizes: 423 nm (solid), 455 nm (dashed), 495 nm (dotted), 553 nm (dash-dot), and 649 nm (dash-dot-dot). The absorption bands are at 934 nm, 980 nm, 1083 nm, 1224 nm, and 1416 nm, respectively. The optical absorption bands are consistent with the SEM measurements.

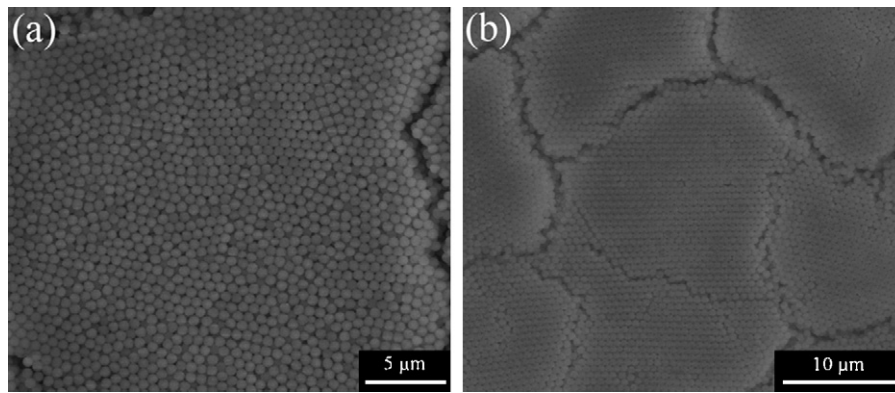


**Fig. 9.** SEM images of self-assembled colloidal photonic crystals formed on horizontal glass slides with different evaporation temperatures: (a) 40 °C and (b) 80 °C. The mean diameter of VFSSs is 649 nm.

ing to

$$n_{\text{eff}} = \sqrt{n_s^2 f + n_a^2 (1-f)} = \sqrt{1.445^2 \times 0.74 + 1 \times 0.26} \approx 1.344 \quad (4)$$

According to Eqs. (2)–(4), finally we get

$$\lambda_{\text{max}} = 2.193D \quad (5)$$

Bragg peaks ( $\lambda_{\text{max}}$ ) got from SEM measurements using Eq. (5), the optical transmission spectra observed absorption bands ( $\lambda$ ), and the deviations  $\delta = ((\lambda - \lambda_{\text{max}})/\lambda_{\text{max}}) \times 100\%$  were listed in Table 2. The deviations  $\delta$  are all less than  $\pm 2\%$ . The optical measurements are consistent with the microstructure obtained.

### 3.5. Influence of evaporation temperature on colloidal photonic crystals

The samples were fabricated at different evaporation temperatures to evaluate the effect of the evaporation temperature on the crystalline quality of colloidal photonic crystals. Fig. 9 shows self-assembled colloidal photonic crystals composed of 649 nm VFSSs formed on horizontal glass slides. For the sample with lower temperature (40 °C), the arrangements are incompact, and few consecutive periodic arrays could be seen; for the sample with higher temperature (80 °C), the arrangements are compact, but the cracks are more than the sample assembled at 60 °C (see Fig. 5).

As discussed in Section 3.3, the Gibbs free energy difference between *fcc* and *hcp* is 0.005RT per mol [37]. The higher the evaporation *T*, the larger the free energy difference is, and this could be responsible for the tendency to the *fcc* phase. For samples fabricated at a higher evaporation temperature condition, the VFSSs have more kinetic energy to sample many possible lattice sites, so the defects will be reduced. However, the evaporation temperature cannot be too high, because a higher evaporation temperature will lead to a faster evaporation rate, i.e., a higher crystal growth rate [41]. Faster evaporation leads to faster array formation, so the VFSSs do not have sufficient time to find suitable lattice sites, thus the defects were formed. Furthermore, faster evaporation rate

**Table 2**

Bragg peaks ( $\lambda_{\text{max}}$ ) of different particle sizes (*D*), transmission absorption bands ( $\lambda$ ), and deviation ( $\delta$ ).

Sample	<i>D</i> (nm)	$\lambda_{\text{max}}$ (nm)	$\lambda$ (nm)	$\delta$
1	649	1423	1416	−0.51
2	553	1213	1224	0.93
3	495	1086	1083	−0.23
4	455	998	980	−1.79
5	423	928	934	0.69

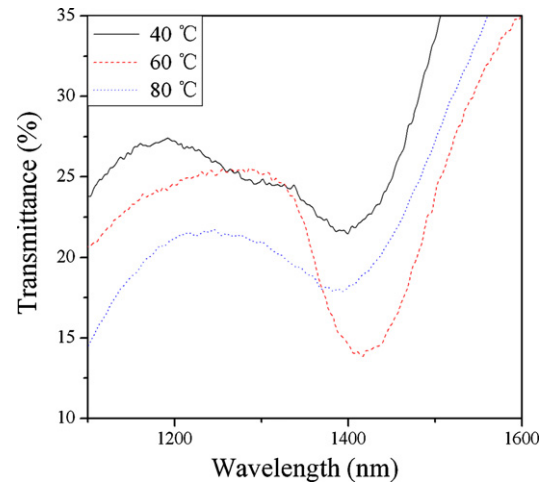


**Fig. 10.** Transmission spectra at normal incidence for colloidal photonic crystals prepared at 40 °C (solid), 60 °C (dashed), and 80 °C (dotted). The absorption bands are at 1399 nm, 1416 nm, and 1394 nm, respectively. The Bragg peak has a blue shift when the evaporation temperature is too high or too low.

increases the surface tension in thin colloidal films, leading to the formation of cracks in the 3D colloidal photonic crystals. These are consistent with the previous report that a longer crystallization time can lead to the better tendency to *fcc* structure from gravity sedimentation experiments, as the spheres have time to find low-potential sites [42].

Fig. 10 shows transmission spectra of the as-prepared 3D colloidal photonic crystals with different evaporation temperatures. The solid, dashed, and dotted lines represent the sample fabricated at 40 °C, 60 °C, and 80 °C. The absorption bands are at 1399 nm, 1416 nm, and 1394 nm, respectively. Due to the samples are lowly ordered at 40 °C and 80 °C, their stop bands broaden and attenuate compared with the stop band fabricated at 60 °C. It must be noted that the stop band has a blue shift about 20 nm at 40 °C and 80 °C. This may be attributed to looser stacking (large spheres separation) and the existence of more disorder and cracks in the film.

## 4. Summary

We have demonstrated an effective and reproducible method for the controlled synthesis of highly monodisperse VFSSs in aqueous solution. This method is remarkable for its simplicity (*one process, one precursor and one solvent*); for its good control of the size, uniformity and stability of hybrid silica spheres; and for its self-hydrolysis ability to realize homogeneous nucleation of silica, fast reaction and reproducibility. The size of hybrid silica

spheres could be adjusted from 420 to 650 nm with  $\sigma_r$  below 2% by controlling the dripping speed of diluted ammonia catalyst, without changing the concentration of precursor/catalyst. The dripping speed has to be higher than 30 drops/min in order to make the reaction proceed successfully. The increasing of the dripping speed has a reverse effect on the particle size. The VFSSs could be used as fabrication of colloidal photonic crystals by a simple gravity sedimentation process. And the resulted periodic arrays exhibit good optical properties. The knowledge gained from this study will be useful and convenient in the design and preparation of organic–inorganic hybrid materials especially in monodisperse surface-modified silica spheres. The highly monodisperse hybrid silica spheres are expected to find more uses as biocatalyst, surface modification, and assembly of colloidal photonic crystals.

## Acknowledgments

We are grateful for the support from the MOST of China (2007CB936204) and the NSFC (50672002 and 60771002). We are also thankful for Drs. L. Chen and J. Chen for the help on the ESEM and TEM operation at physical laboratory of microscopy.

## References

- [1] E. Yablonovitch, Inhibited spontaneous emission in solid-state physics and electronics, *Phys. Rev. Lett.* 58 (1987) 2059–2062.
- [2] S. John, Strong localization of photons in certain disordered dielectric superlattices, *Phys. Rev. Lett.* 58 (1987) 2486–2489.
- [3] C. López, Materials aspects of photonics crystals, *Adv. Mater.* 15 (2003) 1679–1704.
- [4] D.J. Norris, Y.A. Vlasov, Chemical approaches to three-dimensional semiconductor photonic crystals, *Adv. Mater.* 13 (2001) 371–376.
- [5] K. Busch, G. Freymann, S. Linden, S.F. Mingaleev, L. Tkeshelashvili, M. Wegener, Periodic nanostructures for photonics, *Phys. Rep.* 444 (2007) 101–202.
- [6] M. Campbell, D.N. Sharp, M.T. Harrison, R.G. Denning, A.J. Turberfield, Fabrication of photonic crystals for the visible spectrum by holographic lithography, *Nature* 404 (2000) 53–56.
- [7] E. Vekris, V. Kitaev, G. Freymann, D.D. Perovic, J.S. Aitchison, G.A. Ozin, Buried linear extrinsic defects in colloidal photonic crystals, *Adv. Mater.* 17 (2005) 1269–1272.
- [8] Q. Yan, L. Wang, X.S. Zhao, Artificial defect engineering in three-dimensional colloidal photonic crystals, *Adv. Funct. Mater.* 17 (2007) 3695–3706.
- [9] E.C. Nelson, F.G. Santamaría, P.V. Braun, Lattice-registered two-photon polymerized features within colloidal photonic crystals and their optical properties, *Adv. Funct. Mater.* 18 (2008) 1983–1989.
- [10] Y. Xia, B. Gates, Y. Yin, Y. Lu, Monodispersed colloidal spheres: old materials with new applications, *Adv. Mater.* 12 (2000) 693–713.
- [11] A. Blanco, E. Chomski, S. Grabtchak, M. Ibisate, S. John, S.W. Leonard, C. López, F. Meseguer, H. Míguez, J.P. Mondia, G.A. Ozin, O. Toader, H.M. Driel, Large-scale synthesis of a silicon photonic crystal with a complete three-dimensional bandgap near 1.5 micrometres, *Nature* 405 (2000) 437–440.
- [12] B.H. Juárez, P.D. García, D. Golmayo, A. Blanco, C. López, ZnO inverse opals by chemical vapor deposition, *Adv. Mater.* 17 (2005) 2761–2765.
- [13] Y.S. Lin, Y. Hung, H.Y. Lin, Y.H. Tseng, Y.F. Chen, C.Y. Mou, Photonic crystals from monodisperse lanthanide-hydroxide-at-silica core/shell colloidal spheres, *Adv. Mater.* 19 (2007) 577–580.
- [14] G.I.N. Waterhouse, J.B. Metson, H. Idriss, D. Sun, Physical and optical properties of inverse opal  $\text{CeO}_2$  photonic crystals, *Chem. Mater.* 20 (2008) 1183–1190.
- [15] P. Jiang, J.F. Bertone, K.S. Hwang, V.L. Colvin, Single-crystal colloidal multilayers of controlled thickness, *Chem. Mater.* 11 (1999) 2132–2140.
- [16] S. Wong, V. Kitaev, G.A. Ozin, Colloidal crystal films: advances in universality and perfection, *J. Am. Chem. Soc.* 125 (2003) 15589–15598.
- [17] W. Stöber, A. Fink, E. Bohn, Controlled growth of monodisperse silica spheres in micron size range, *J. Colloid Interface Sci.* 26 (1968) 62–66.
- [18] W. Wang, B. Gu, L. Liang, W.A. Hamilton, Fabrication of near-infrared photonic crystals using highly-monodispersed submicrometer  $\text{SiO}_2$  spheres, *J. Phys. Chem. B* 107 (2003) 12113–12117.
- [19] W. Wang, B. Gu, L. Liang, W.A. Hamilton, Fabrication of two- and three-dimensional silica nanocolloidal particle arrays, *J. Phys. Chem. B* 107 (2003) 3400–3404.
- [20] W. Wang, B. Gu, Self-assembly of two- and three-dimensional particle arrays by manipulating the hydrophobicity of silica nanospheres, *J. Phys. Chem. B* 109 (2005) 22175–22180.
- [21] A.S.M. Chong, X.S. Zhao, Functionalized nanoporous silicas for the immobilization of penicillin acylase, *Appl. Surf. Sci.* 237 (2004) 398–404.
- [22] V. Uricanu, D. Donescu, A.G. Banu, S. Serban, M. Olteanu, M. Dudau, Organic–inorganic hybrids made from polymerizable precursors, *Mater. Chem. Phys.* 85 (2004) 120–130.
- [23] Z.J. Wu, H. Han, W. Han, B. Kim, K.H. Ahn, K. Lee, Controlling the hydrophobicity of submicrometer silica spheres via surface modification for nanocomposite applications, *Langmuir* 23 (2007) 7799–7803.
- [24] W. Wang, B. Gu, L. Liang, Effect of anionic surfactants on synthesis and self-assembly of silica colloidal nanoparticles, *J. Colloid Interface Sci.* 313 (2007) 169–173.
- [25] E.J. Nassar, E.C.O. Nassor, L.R. Ávila, P.F.S. Pereira, A. Cestari, L.M. Luz, K.J. Ciuffi, P.S. Calefi, Spherical hybrid silica particles modified by methacrylate groups, *J. Sol–Gel Sci. Technol.* 43 (2007) 21–26.
- [26] H.J. Hah, J.S. Kim, B.J. Jeon, S.M. Koo, Y.E. Lee, Simple preparation of monodisperse hollow silica particles without using templates, *Chem. Commun.* (2003) 1712–1713.
- [27] Y.G. Lee, J.H. Park, C. Oh, S.G. Oh, Y.C. Kim, Preparation of highly monodispersed of hybrid silica spheres using a one-step sol–gel reaction in aqueous solution, *Langmuir* 22 (2007) 10875–10879.
- [28] S. Sankaraiyah, J.M. Lee, J.H. Kim, S.W. Choi, Preparation and characterization of surface-functionalized polysilsesquioxane hard spheres in aqueous medium, *Macromolecules* 41 (2008) 6195–6204.
- [29] T.S. Deng, Q.F. Zhang, J.Y. Zhang, X. Shen, K.T. Zhu, J.L. Wu, One-step synthesis of highly monodisperse hybrid silica spheres in aqueous solution, *J. Colloid Interface Sci.* 329 (2009) 292–299.
- [30] D.W. Sendorf, G.E. Maciel, Solid-state NMR studies of the reactions of silica surfaces with polyfunctional chloromethylsilanes and ethoxymethylsilanes, *J. Am. Chem. Soc.* 105 (1983) 3767–3776.
- [31] I. Chuang, D.R. Kinney, G.E. Maciel, Interior hydroxyls of the silica gel system as studied by  $^{29}\text{Si}$  CP-MAS NMR spectroscopy, *J. Am. Chem. Soc.* 115 (1993) 8695–8705.
- [32] M.P. Vinod, D. Bahenemann, P.R. Rajamohanam, K. Vijayamohanam, A novel luminescent functionalized siloxane polymer, *J. Phys. Chem. B* 107 (2003) 11583–11588.
- [33] S. Jain, J.G.P. Goossens, M. Duin, Synthesis, characterization and properties of (vinyl triethoxy silane-grafted PP)/silica nanocomposites, *Macromol. Symp.* 233 (2006) 225–234.
- [34] C.J. Brinker, G.W. Scherer, *Sol–Gel Science: The Physics and Chemistry of Sol–Gel Processing*, Academic, San Diego, 1990.
- [35] H. Míguez, F. Meseguer, C. López, A. Mifsud, J.S. Moya, L. Vázquez, Evidence of FCC crystallization of  $\text{SiO}_2$  nanospheres, *Langmuir* 13 (1997) 6009–6011.
- [36] Z.Z. Gu, A. Fujishima, O. Sato, Fabrication of high-quality opal films with controllable thickness, *Langmuir* 14 (2002) 760–765.
- [37] L.V. Woodcock, Entropy difference between the face-centred cubic and hexagonal close-packed crystal structures, *Nature* 385 (1997) 141–143.
- [38] A.D. Bruce, N.B. Wilding, G.J. Ackland, Free energy of crystalline solids: a lattice-switch Monte Carlo method, *Phys. Rev. Lett.* 79 (1997) 3002–3005.
- [39] H. Míguez, C. López, F. Meseguer, A. Blanco, L. Vázquez, R. Mayoral, M. Ocaña, V. Fornés, A. Mifsud, Photonic crystal properties of packed submicrometric  $\text{SiO}_2$  spheres, *Appl. Phys. Lett.* 71 (1997) 1148–1150.
- [40] A. Richel, N.P. Johnson, D.W. McComb, Observation of Bragg reflection in photonic crystals synthesized from air spheres in a titania matrix, *Appl. Phys. Lett.* 76 (2000) 1816–1818.
- [41] Y.H. Ye, F. LeBlanc, A. Haché, V.V. Truong, Self-assembling three-dimensional colloidal photonic crystal structure with high crystalline quality, *Appl. Phys. Lett.* 78 (2001) 52–54.
- [42] C. Dux, H. Versmold, Light diffraction from shear ordered colloidal dispersions, *Phys. Rev. Lett.* 78 (1997) 1811–1814.